The Role of Photomask Resolution on the Performance of Arrayed-Waveguide Grating Devices

Chauhan D. Lee, Wei Chen, Qiang Wang, Yung-Jui Chen, *Senior Member, IEEE*, Warren T. Beard, *Member, IEEE*, Dennis Stone, Robert F. Smith, Rod Mincher, and Ian R. Stewart

***Abstract*—The crosstalk performance of an arrayed-waveguide grating (AWG) multiplexer or demultiplexer is primarily caused by random optical phase errors introduced in the arrayed waveguides. Because the layout of waveguides on a wafer is patterned via photomask through the photolithography process, the resolution of a photomask has a direct influence on the phase errors of an AWG. This paper presents a theoretical analysis on the phase error caused by photomask resolution and other basic design parameters. Both calculation and measurement results show that a high-resolution photomask (better than 25 nm) is a critical requirement to produce low-crosstalk (less than −30 dB) AWG demultiplexers. We also investigate the effect of nonideal power distribution in the arrayed waveguides because it contributes considerable phase errors when material impurity is not well controlled during wafer fabrication. Basic criteria of power profile truncation, number of grating waveguides, and material index variation are also summarized.**

***Index Terms*—Arrayed-waveguide grating (AWG), optical crosstalk, optical phase error, planar lightwave circuits (PLCs).**

I. INTRODUCTION

WITH the rapid increase of channel counts in dense wavelength division multiplexing (DWDM) systems, integrated arrayed-waveguide grating (AWG) devices are attractive and essential components for various applications requiring wavelength multiplexing–demultiplexing functions [1]. The design and fabrication issues relevant to the performance of AWG devices, especially optical crosstalk, are of great interest and importance.

The passband property of an AWG demultiplexer is mainly a result of phase-front interference of light propagating along all arrayed waveguides with constant length difference among them [2]–[4]. Thus, the extinction ratio (i.e., crosstalk) is directly affected by any deviation from the ideal path lengths of those waveguides during the fabrication process. This deviation, often quoted as phase error, needs to be considerably small in order to yield a good crosstalk figure and, to a less extent, good throughput [5]. The path-length control, apart from material and process variation, is determined primarily by photolithography. Currently, with photomask resolution ranging from 25 nm to 250 nm, considerable path-length variation can result from the photomask itself. Aside from waveguide fabrication methods and material purity control of wafer manufacturing, the photomask resolution has long been considered a significant contributor to path length deviation and, consequently, a key element determining the crosstalk performance. However, only limited studies have investigated this important subject so far [6], [7]. In this paper, we present a detailed study of the photomask resolution effect along with other basic design parameters. We compare the simulation results with actual passband spectrum and phase-error measurement data of devices fabricated using photomasks of different resolutions. The simulation results fit our measured data quite well and provide excellent guidelines in choosing design parameters and mask resolution for AWG devices of various performance requirements.

In our simulation, an AWG demultiplexer is presented as a series of waveguides, each with different path lengths and bearing different electromagnetic-field amplitude and phase. The path lengths are set to designed values, with constant length difference between adjacent waveguides, plus a Gaussian-distributed random phase error with an assigned standard deviation. For each given distribution of path lengths, the simulation program constructs the output-demultiplexed passband spectrum and calculates the associated crosstalk. The simulation process yields a calculated data point representing the relationship between crosstalk and standard deviation of path-length error. By adding many sampling points (different deviation values) to the graph, we obtain a clear trend statistically.

We have measured the phase errors of fabricated AWG demultiplexers using low coherent source Fourier transform spectroscopy [3]–[5] to compare with calculated results. The resolution of our phase error measurements is 1°, which corresponds to 5 nm in path length. This is well within an acceptable range of accuracy when compared to the 25- to 100-nm photomask resolution used in fabricating our real devices. This accuracy can also be verified by comparing a reconstructed passband spectrum from measured phase data to one measured by an optical spectrum analyzer.

II. MODELING AND SIMULATION

A. Theory and Performance Determining Factors of AWGs

Fig. 1 schematically shows the layout of an AWG multiplexer–demultiplexer. This AWG device is composed of input–output waveguides, two focusing slab regions, and an array of waveguides with constant path-length difference ΔL between adjacent channels. The principles of multiplexing and demultiplexing in an AWG device are the same, except

Manuscript received February 15, 2001; revised June 26, 2001.

C. D. Lee, W. Chen, Q. Wang, and Y.-J. Chen are with the Computer Science and Electronic Engineering Department, University of Maryland, Baltimore, MD 21250 USA.

W. T. Beard and D. Stone are with the Laboratory for Physical Sciences, University of Maryland, College Park, MD 20742 USA.

R. F. Smith, R. Mincher, and I. R. Stewart are with the Department of Defense, Fort Meade, MD 20755 USA.

Publisher Item Identifier S 0733-8724(01)09641-4.

0733–8724/01$10.00 © 2001 IEEE

Authorized licensed use limited to: Johns Hopkins University. Downloaded on November 6, 2008 at 19:40 from IEEE Xplore. Restrictions apply.

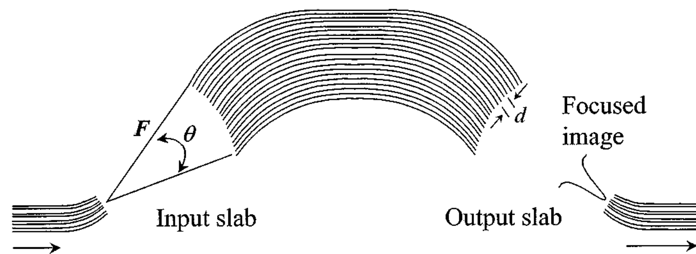

Fig. 1. Schematic diagram of an AWG demultiplexer.

that the direction of propagating light is reversed. In a demultiplexer mode, light passing through an input waveguide enters into the input slab region and propagates divergently. The far field of the diffracted light in the slab waveguide is a Gaussian-like pattern with a circular wavefront of constant phase. The arrayed waveguides at the input side are arranged on the circle centered at the junction between the central-input waveguide and the slab waveguide. The radius of this circle is known as the focal length of the slab region F. The divergent field is then coupled into each of the arrayed waveguides with equal phase. Every waveguide in the array is located along the circle with a constant separation (grating pitch d) along the chord. Multiple input–output waveguides are connected to the two slab regions along the focal plane in order to construct a symmetric one-to-one imaging system. This arrangement is known as the Rowland Circle configuration. The constant path-length difference ΔL produces a constant phase difference between neighboring waveguides. Each waveguide's optical field propagates to the output slab region and interferes with one another to form an image of the input optical field, which is focused to an output waveguide according to the designed wavelength.

Consequently, the fidelity of the focused output image determines the crosstalk performance of an AWG and is, thus, affected by phase errors introduced in the arrayed waveguides. In the following discussion, we assume the field profile and waveguide spacing of the input–output waveguides are properly designed and will not introduce noticeable crosstalk. There are a number of causes for optical phase errors. First of all, the deposition process of different glass layers of a silica waveguide wafer introduces material-index fluctuations and thickness variations. The index fluctuation is numerically estimated by Takashi *et al.* [7], and our measurement shows a nominal equivalent path-length error of about 2 nm (for an AWG chip area) for a design with $\Delta L = 42\ \mu$m. The second cause of phase errors is due to the imperfections that result from the photolithography and waveguide etching process. The height and width of a waveguide cannot be perfectly produced throughout this processing. Using the beam propagation method (BPM), our calculations show that the variation of modal effective index is about 0.000 45/μm due to the error of the height and width of a 6 μm $\times$ 6 μm waveguide. Third, because the path-length error caused by the writing (e-beam or laser) resolution of a photomask is directly transferred on to a wafer during the photolithography process, we believe that photomask resolution is the most significant contributor to optical phase errors. The comparison of the influence from the above three causes are shown in Table I with their equivalent path-length errors.

B. Simulation Method

The passband spectrum of an AWG device is described by

$$P(\lambda) = |I(\lambda)|^2 = \left| \sum_n h_n e^{-i\frac{2\pi}{\lambda} n_c x_n} \right|^2 \tag{1}$$

where $P(\lambda)$ is the optical power spectrum, $I(\lambda)$ is the field spectrum, n_c is the effective index of arrayed-waveguides, h_n is the normalized field amplitude at the nth grating waveguide, and x_n is the optical path length. Assuming

$$h_n = (h_n)_{\text{design}} + \Delta h_n, \quad \text{and} \quad x_n = (x_n)_{\text{design}} + \Delta x_n \tag{2}$$

where $(h_n)_{\text{design}}$ is the ideal value of h_n, and $(x_n)_{\text{design}}$ is the ideal design values of x_n that are evenly spaced with a constant path-length difference ΔL. Once the diffraction order m and operating center wavelength λ_c of an AWG demultiplexer are determined, ΔL is equal to $m\lambda_c$. The path-length error Δx_n and power fluctuation Δh_n are both Gaussian-distributed errors with assigned standard deviations. The standard deviation of Δx_n is simply the writing resolution of a photomask for all calculations. In reality, this value should be determined by statistical measurement results of fabricated devices. We neglect the errors caused by imperfect width and material index of the grating waveguides because they are comparatively small. Having each set of generated x and h, we can treat them as a representation of an AWG demultiplexer device. Simply applying (1), one can construct output transmission spectra at the wavelengths of interest and calculate crosstalk values as well. Using the Monte Carlo method, we generate numerous calculated results and plot them on different graphs of crosstalk values versus various design parameters to clearly illustrate the trend of crosstalk performance.

In our simulation, we use the following parameters from our AWG design rules and compare them with actual measurement results of fabricated devices. Photomask resolution is the first and most important parameter considered in this paper. We translate this resolution into the statistical standard deviation of waveguide path-length error distribution. The photomask resolution is set from 5 nm to 100 nm, which covers the current achievable and emerging technology for the coming years. Second, the number of grating waveguides N_g within the collected power profile is also an important factor in constructing low-crosstalk output transmission spectra by interference effect. This value is obtained by selecting appropriate grating pitch d and focal length F of the slab region according to $N_g = 2F\sin(\theta/2)/d + 1$. Notice that the spacing of the output waveguides is proportional to the focal length F, as well [8], [9], when the independent demultiplexer parameters (wavelength spacing, center wavelength, and free spectral range) are fixed. Theoretically, using more grating waveguides is preferable for achieving lower crosstalk if the material property and waveguides are perfect. However, one should consider the issues such as chip size and material uniformity to

Authorized licensed use limited to: Johns Hopkins University. Downloaded on November 6, 2008 at 19:40 from IEEE Xplore. Restrictions apply.

TABLE I
COMPARISON OF DIFFERENT CAUSES OF PATH-LENGTH ERROR

Causes	Influence	Maximum equivalent path-length error (nm)
Index fluctuation	2.7×10^{-5}	≅ 1.7 (for ΔL = 42 μm)
Waveguide width/height	4.5×10^{-4}/μm (index change)	≅ 4 (assuming 0.2 um maximum error on width/height)
Photomask resolution	25 nm-100 nm	≅ 25-100

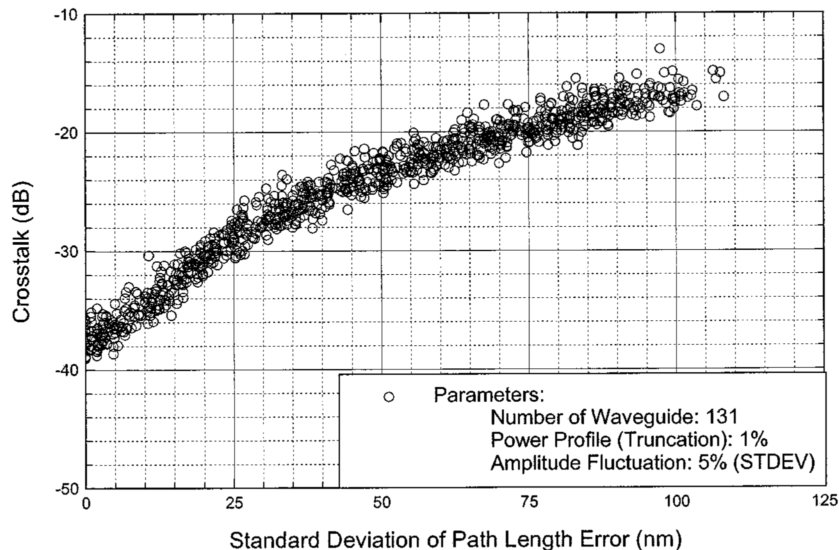

Fig. 2. Crosstalk variation due to path-length error.

determine a practical number when designing AWG devices. The third parameter is the power profile to be collected at the junction of the input slab region and the grating waveguides, or, equivalently, the divergent angle θ shown in Fig. 1. It is often quoted as a percentage ratio between the power of the outermost waveguide and the center waveguide. The value is about 1% (in power) for a typical design. The last parameter is the fluctuation of field amplitudes in the waveguide array. Ideally, the amplitude values should be a Gaussian-like distribution along these grating waveguides. For other applications that require a different grating design, one can also use a non-Gaussian type of distribution functions to analyze the crosstalk performance. To our best understanding, this error is mostly material and manufacturing process related. An estimated 5% fluctuation (Δh_n), which agrees with our measurement results, is used in most of the calculations to reflect current performance of our AWG devices. All calculations are based on the design for a 16-channel 200-GHz spacing (FSR $=$ 4800 GHz) AWG demultiplexer with waveguide core size of 6 μm $\times$ 6 μm and 0.75% index difference.

C. Simulation Results

1) Influence on Crosstalk by Path-Length Error: Fig. 2 is a statistical plot of simulated crosstalk versus path-length error with certain design parameters. Each dot on the graph represents a crosstalk value of output transmission spectra of a simulated AWG demultiplexer. As we can see, -25 dB of crosstalk is achievable when the standard deviation of path-length error, i.e., effective photomask resolution, is about 50 nm; -30 dB of crosstalk is achievable when the standard deviation of path-length error is about 25 nm. Notice that the other fixed parameters are the number of grating waveguides (131), collected power profile (up to 1%), and field-amplitude fluctuation (5%). The reduction of crosstalk can be more than 10 dB just by improving the path-length error from 100 nm to 25 nm, and even more with less path-length error. This dominant trend of crosstalk reduction cannot be obtained by changing other parameters, as we will show in the following calculations. Although the statistical trend is self-explanatory, we also examine how other design parameters affect the crosstalk performance.

2) Influence on Crosstalk by Number of Waveguides: The influence by number of grating waveguides is shown in Fig. 3. Changing the number of grating waveguides is equivalent to changing the grating pitch or focal length of an AWG design. Once the divergent angle θ (see Fig. 1) is determined, reducing the grating pitch d or increasing the focal length F demands more grating waveguides to collect the same amount of power. In order to distinguish the different statistical dot-array clearly, we average the dot array to produce the smoothed curves shown in Fig. 3(b).

In accordance with the theory of diffraction gratings, adding more grating waveguides (using larger focal length or smaller grating pitch) improves the crosstalk performance, as shown in

Authorized licensed use limited to: Johns Hopkins University. Downloaded on November 6, 2008 at 19:40 from IEEE Xplore. Restrictions apply.

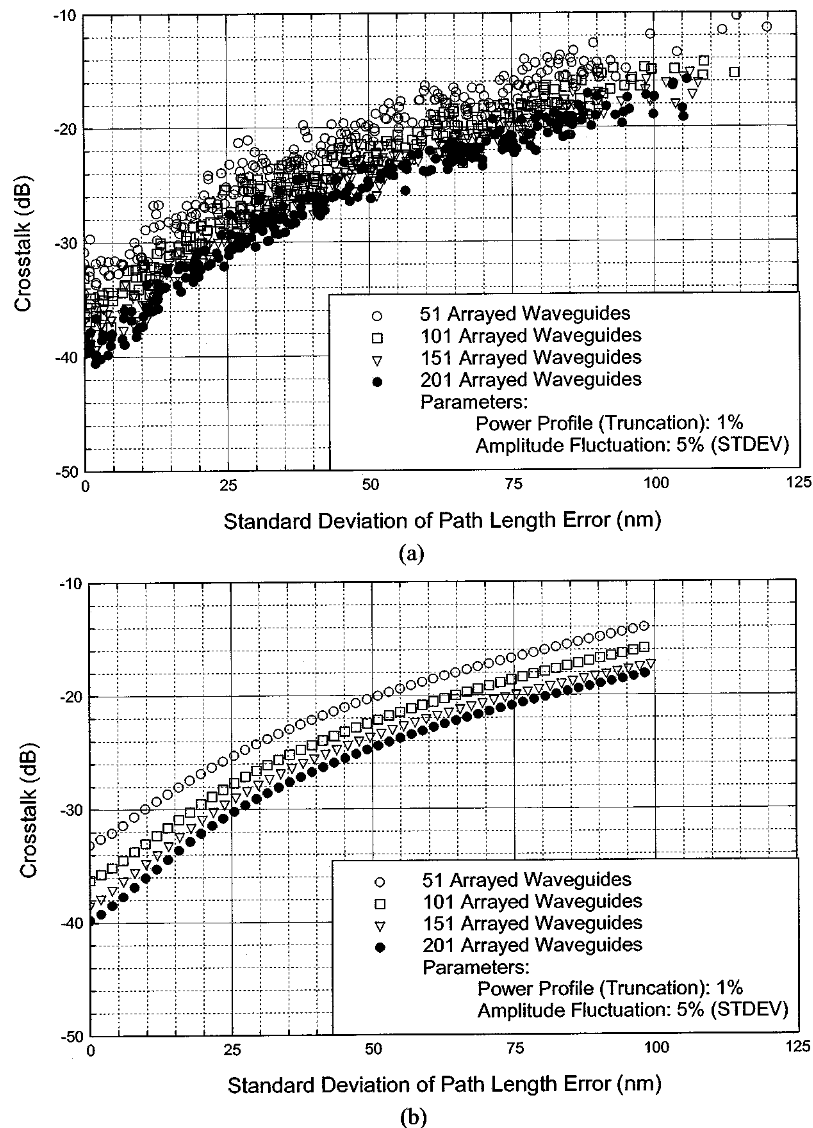

Fig. 3. Effect of number of grating waveguides.

Fig. 3. However, increasing the number of grating waveguides not only requires larger chip size but also introduces more unavoidable phase and amplitude errors caused by imperfect optical properties of waveguides, e.g., variations of material index, waveguide core size, etc. An optimized number must be determined experimentally with the consideration of device yield per wafer and fabrication technologies.

3) Influence on Crosstalk by Power Truncation: By using a limited number of grating waveguides at the input slab region, the AWG can only collect a fraction of the input optical power. This leads to the power truncation issue. Fig. 4 shows an averaged result of the power profile influence on crosstalk with 10 devices per point. The values of grating pitch and focal length are fixed parameters for this calculation. The change in the number of waveguides changes the amount of collected power from the input slab region as well. We notice that the crosstalk reduction is more effective when one widens the coverage of input power profile and uses a photomask resolution higher than 25 nm. When the path-length error is greater than 30 nm, the crosstalk caused by power truncation becomes less distinguishable.

4) Influence on Crosstalk by Amplitude Fluctuation: There are two main causes of field amplitude fluctuation, the refractive index nonuniformity in the two slab regions and the imperfections in the grating waveguides. Any impurity and index variation in the slab regions can distort the Gaussian field profile of light propagating in these regions and, therefore, introduce amplitude fluctuation when coupling into the grating waveguides. Each of these waveguides can also have different losses due to different bending radii and fabrication errors. By improving the purity of waveguide material and reducing processing induced variations, and, thus, less amplitude fluctuation in grating waveguides, one can obtain obvious crosstalk reduction using higher resolution photomask, as seen in Fig. 5. The amplitude fluctuation should be as small as possible. Typically, 5% is the basic requirement for a high performance device. However, if path-length error is greater than 50 nm (low photomask resolution), better material purity and wafer fabrication process (less

Authorized licensed use limited to: Johns Hopkins University. Downloaded on November 6, 2008 at 19:40 from IEEE Xplore. Restrictions apply.

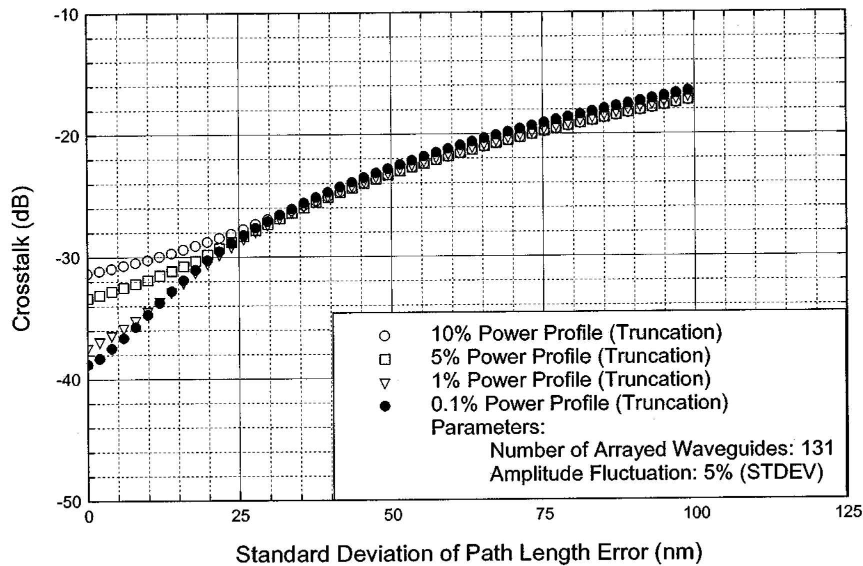

Fig. 4. Power truncation effect on crosstalk performance.

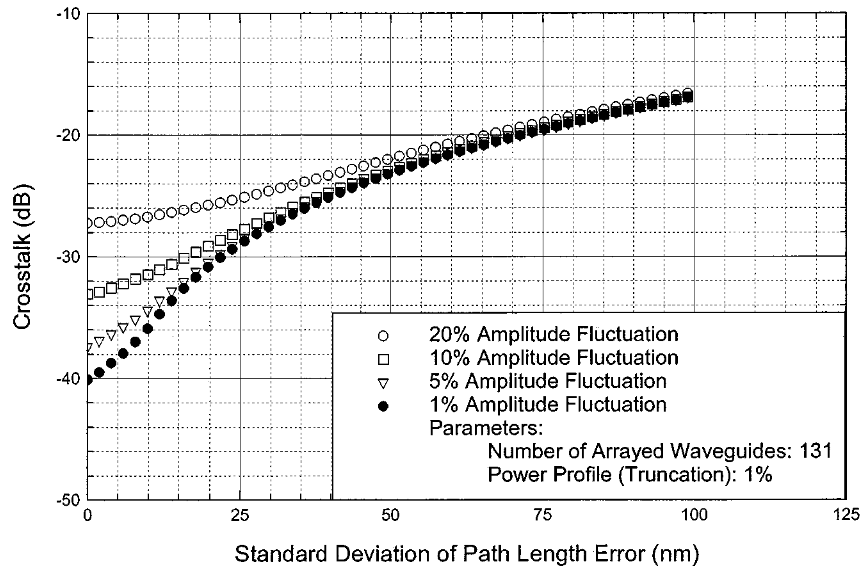

Fig. 5. Crosstalk due to power fluctuation in grating waveguides.

amplitude fluctuation) will contribute little toward crosstalk reduction. Again, a major improvement is shown as we reduce the path-length error. If a crosstalk value lower than -35 dB is a required specification, while effective photomask resolution is already better than 25 nm, one must improve the amplitude fluctuation, as well, for consistent results.

5) Ideal Case: For comparison, crosstalk caused only by path-length error (photomask resolution) is shown in Fig. 6. In this calculation, we assume perfect waveguide material and no power fluctuation in the grating waveguides. Each point represents an average value of 10 simulated devices. When effective photomask resolution is higher than 25 nm, crosstalk values start to drop more noticeably, as shown in this figure. Increasing the number of waveguides (smaller grating pitch or larger focal length) contributes to similar crosstalk improvement, as shown in Fig. 3. Major differences occurs in the shorter path-length error (less than 15 nm) region, where the case of 0% amplitude fluctuation has much lower crosstalk than the 5% fluctuation case shown in Fig. 3.

III. Experimental Investigation

A. Index Variation

By measuring the central wavelength of each AWG device on a wafer, one can readily calculate the effective waveguide index variation on the wafer using the equation $N_c = m \cdot \lambda_c/\Delta L$. Table II and Fig. 7 show a typical waveguide index variation of 12 AWG demultiplexers on a 5-in wafer. The standard deviation of the index variation on the whole wafer is roughly 2×10^{-4}. For a single device, this variation can be estimated as proportional to the area of the arrayed waveguides region versus the whole wafer (0.5 in $\times$ 0.25 in/3.7 in $\times$ 2.5 in). The estimated index error for a single device is 2.7 $\times10^{-5}$, which is equivalent to 1.7-nm optical path error on an AWG design with

Authorized licensed use limited to: Johns Hopkins University. Downloaded on November 6, 2008 at 19:40 from IEEE Xplore. Restrictions apply.

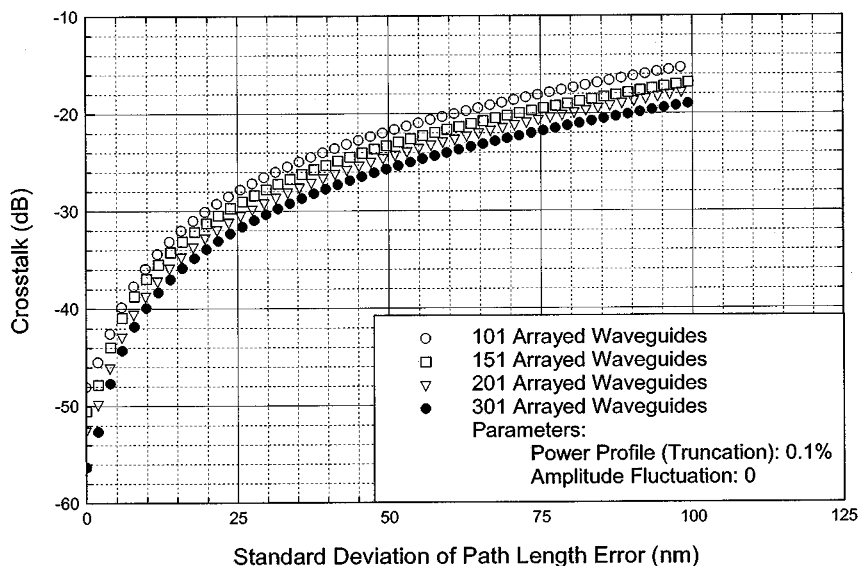

Fig. 6. Crosstalk performance affected only by path-length error due to photomask resolution.

TABLE II
MEASURED EFFECTIVE INDEX

Device	N_c
1a	1.450827
1b	1.450662
2a	1.450497
2b	1.450873
3a	1.450707
3b	1.450657
4a	1.450526
4b	1.450539
5a	1.450586
5b	1.450636
6a	1.451252
6b	1.450640
Average	1.45070015
STDEV	0.00020718

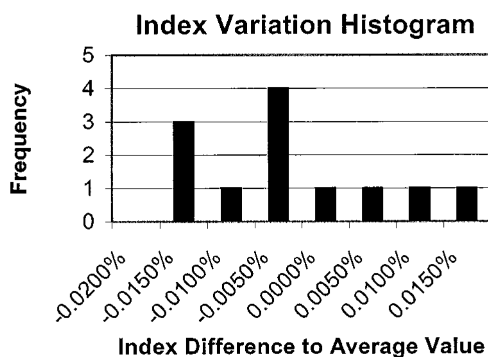

Fig. 7. Index variation histogram on a typical wafer.

$\Delta L = 42\ \mu$m. Compared to errors caused by photomask resolution, it has a much smaller effect on the path-length error.

B. Crosstalk Comparison

Fig. 8 shows a histogram of the crosstalk performance from AWG wafers patterned by different photomask resolutions. A comparison of measured data versus the calculated curve in Fig. 9 shows a good agreement between theoretical simulation and fabricated devices. All of the discussions in this paper have been based on the argument that the optical path error closely corresponds to the photomask resolution. However, we also acknowledge that the better AWG performance results show an optical path error that is smaller than the photomask-resolution value. As a general trend, the two numbers are correlated, as shown in Fig. 9. As mentioned earlier, the real standard deviation of the distribution of path-length error Δx_n should be determined by statistical measurement results from real fabricated devices. In this case, if we apply a fudge factor of 0.7 to the photomask resolution value, that is, the standard deviation of $\Delta x_n = 0.7\times$ photomask resolution, the calculation curve of Fig. 9 fits the best reported AWG results very well. Based on the private information we obtained from different AWG sources, the fudge factor can be as small as 0.5. This fudge factor, which, with no doubt, is material- and processing-dependent, makes sense because the optical exposure process (using an ultraviolet light source) and subsequent high temperature processing steps will tend to smooth out some of the roughness. Improvement of

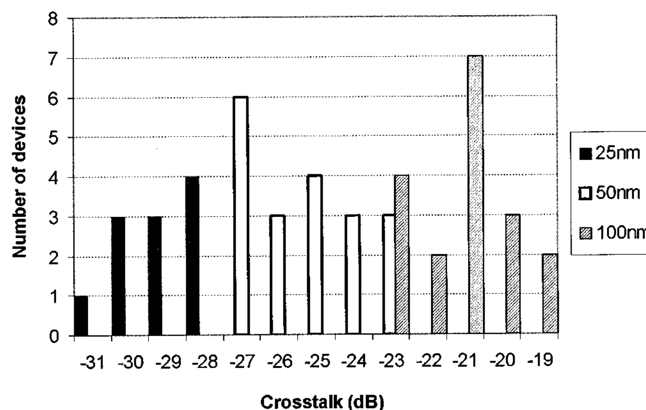

Fig. 8. Histogram of crosstalk performance of AWG devices patterned with different mask resolution.

Authorized licensed use limited to: Johns Hopkins University. Downloaded on November 6, 2008 at 19:40 from IEEE Xplore. Restrictions apply.

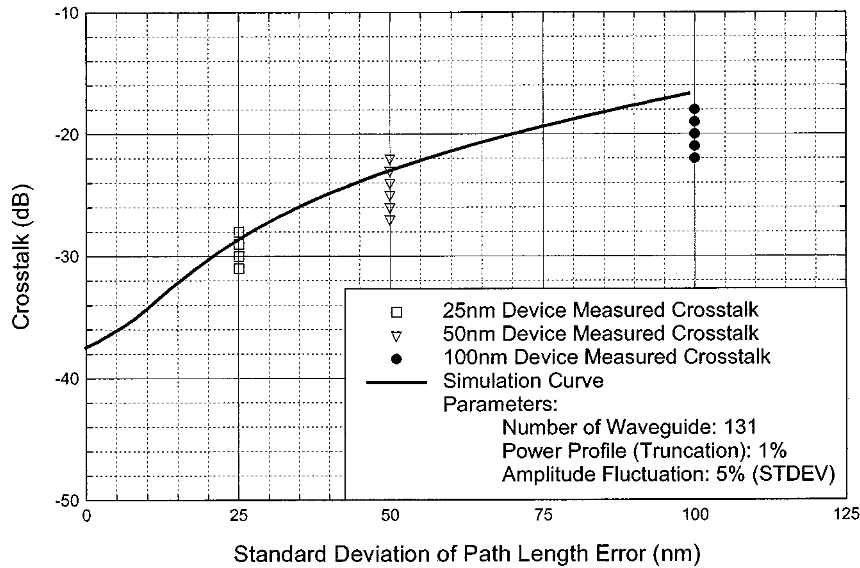

Fig. 9. Measured result versus simulation.

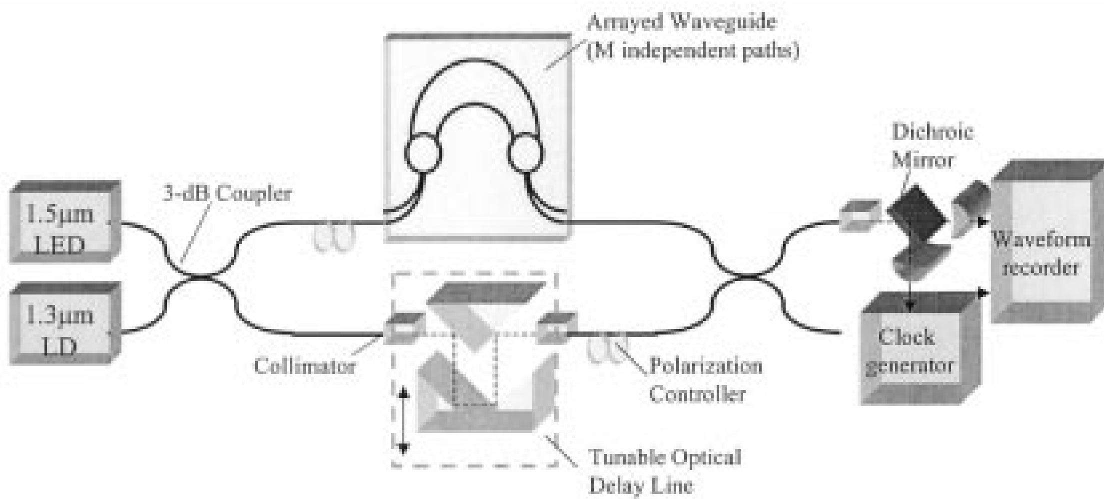

Fig. 10. Low coherent Fourier transform spectroscopy setup for phase error measurement.

photomask writing techniques, waveguide processing, and material properties will reduce the path-length error directly.

C. Phase-Error Measurement

Fig. 10 shows our experimental setup of the low coherent Fourier transform spectroscopy [3]. Using this technique, we can measure both phase and field amplitude in each grating waveguide of an AWG demultiplexer. A typical reconstructed AWG transmission spectrum, according to the phase error measurement, fits very well with the one measured by an optical spectrum analyzer, as shown in Fig. 11. Table III lists the path-length error measured from six AWG demultiplexers patterned by photomasks with different resolutions of 100 nm, 50 nm, and 25 nm. The results show a direct relation among the crosstalk values, path-length error, and photomask resolution. An estimated value of the fudge factor, according to Fig. 9, related to these six devices is around 0.99.

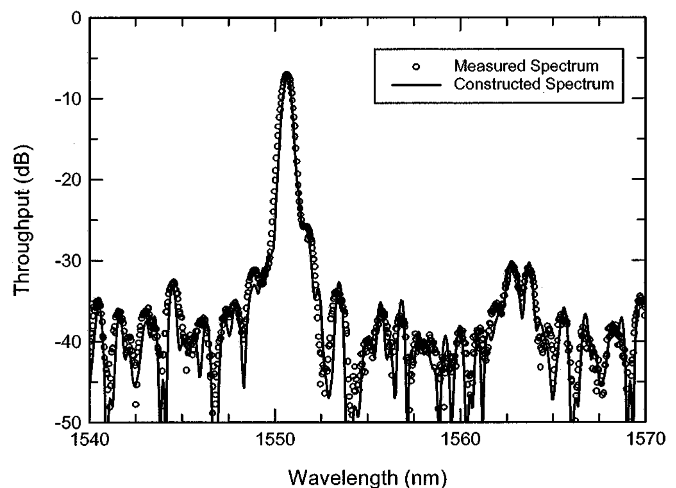

Fig. 11. Throughput spectrum comparison.

Authorized licensed use limited to: Johns Hopkins University. Downloaded on November 6, 2008 at 19:40 from IEEE Xplore. Restrictions apply.

TABLE III
PHASE MEASUREMENT RESULT

Photomask Resolution (nm)	Measured STDEV of Path Length Error (nm)	Fudge Factor
100	92	0.92
100	88	0.88
50	55	1.10
50	51	1.02
25	25	1.00
25	26	1.04

IV. CONCLUSION

We have demonstrated, in the simulation of AWG transmission characteristics, that finite photomask resolution is the major cause of AWG crosstalk problems when other design parameters, such as waveguide geometry, power truncation, and number of grating waveguides, are properly selected. Field-amplitude fluctuation introduced by material impurity and processing imperfection will be a noticeable factor and must be carefully controlled as well. This is particularly true when photomask resolution is better than 25 nm and less than -35 dB crosstalk is required. Using AWG demultiplexers patterned and fabricated by different photomasks, the measured crosstalk performance of all of these devices agreed well with calculated results. All measured transmission spectra are used to verify the precision of data from phase and field amplitude measurements. The match between the values of photomask resolution and path-length error confirms the former as the dominant factor that affects AWG crosstalk performance. By improving the photomask resolution, we believe that the AWG crosstalk performance can be better than -40 dB with necessary path length correction technologies. This is consistent with the state-of-the-art results reported by NTT [9].

REFERENCES

[1] Y. J. Chen and H. Li, "Planar waveguide WDM technology: From components to systems," in *Proc. SPIE*, vol. CR71, 1999, pp. 75–107.
[2] M. K. Smit, "New focusing and dispersive planar component based on an optical phase array," *Electron. Lett.*, vol. 24, pp. 385–386, Mar. 31, 1988.
[3] K. Takada, H. Yamada, and Y. Inoue, "Optical low coherence method for characterizing silica-based arrayed-waveguide grating multiplexers," *J. Lightwave Technol.*, vol. 14, p. 1677, July 1996.
[4] H. Yamada, T. Takada, and M. Seiko, "Crosstalk reduction in a 10-GHz spacing arrayed-waveguide grating by phase-error compensation," *J. Lightwave Technol.*, vol. 16, pp. 364–370, Mar. 1998.
[5] K. Takada, Y. Inoue, H. Yamada, and M. Horiguchi, "Measurement of the phase error distribution in silica-based arrayed-waveguide grating multiplexers by using Fourier transform spectroscopy," *Electron. Lett.*, vol. 30, pp. 1671–1672, Sept. 29, 1994.
[6] K. Takada, H. Yamada, and Y. Inoue, "Origin of channel crosstalk in 100 GHz spaced silica-based arrayed-waveguide grating multiplexer," *Electron. Lett.*, vol. 31, no. 14, pp. 1176–1177, July 1995.
[7] G. Takashi and S. Suzuki, "Estimation of waveguide phase error in silica-based waveguides," *J. Lightwave Technol.*, vol. 15, pp. 2107–2113, Nov. 1997.
[8] M. K. Smit and C. van Dam, "PHASAR-based WDM-devices: Principle, design and applications," *J. Select. Topics Quantum Electron.*, vol. 2, no. 2, pp. 236–250, June 1996.
[9] K. Okamoto, *Fundamentals of Optical Waveguides*. New York: Academic, 2000, ch. 9.

Chauhan D. Lee, photograph and biography not available at the time of publication.

Wei Chen, photograph and biography not available at the time of publication.

Qiang Wang, photograph and biography not available at the time of publication.

Yung-Jui Chen (M'78–SM'90), photograph and biography not available at the time of publication.

Warren T. Beard (S'79–M'80), photograph and biography not available at the time of publication.

Dennis Stone, photograph and biography not available at the time of publication.

Robert F. Smith, photograph and biography not available at the time of publication.

Rod Mincher, photograph and biography not available at the time of publication.

Ian R. Stewart, photograph and biography not available at the time of publication.

Authorized licensed use limited to: Johns Hopkins University. Downloaded on November 6, 2008 at 19:40 from IEEE Xplore. Restrictions apply.